ICE FLOW VELOCITY MAPPING IN EAST ANTARCTICA USING HISTORICAL IMAGES FROM 1960s TO 1980s: RECENT PROGRESS

S. Luo [1,2], Y. Cheng [1,2], Z. Li [1,2], Y. Wang [1,2], K. Wang [1,2], X. Wang [1,2], G. Qiao [1,2], W. Ye [1,2], Y. Li [1,2], M. Xia [1,2], X. Yuan [1,2], Y. Tian [1,2], X. Tong [1,2], R. Li [1,2*]

[1]Center for Spatial Information Science and Sustainable Development Applications, Tongji University, 1239 Siping Road, Shanghai, China - (shulei, chengyuan_1994, tjwkl, wxfjj620, qiaogang, menglianxia, 1996yuanxiaohan, tianyixiang, xhtong, rli) @tongji.edu.cn, (zhenli_0324, yanjunli_1995) @outlook.com, wangyiyu1234567@163.com, yewenkai1990@gmail.com
[2] College of Surveying and Geo-Informatics, Tongji University, 1239 Siping Road, Shanghai, China

Commission TCIII, WG III/9

KEY WORDS: East Antarctica, Ice Flow, Historical Image, Velocity Validation, Ice Flux, Mass Balance

ABSTRACT:

Recent research indicates that the estimated elevation changes and associated mass balance in East Antarctica are of some degree of uncertainty; a light accumulation has occurred in its vast inland regions, while mass loss in Wilkes Land appears significant. It is necessary to study the mass change trend in the context of a long period of the East Antarctic Ice Sheet (EAIS). The input-output method based on surface ice flow velocity and ice thickness is one of the most important ways to estimate the mass balance, which can provide longer-term knowledge of mass balance because of the availability of the early satellites in 1960s. In this study, we briefly describe the method of extracting ice velocity based on the historical optical images from 1960s to 1980s. Based on the draft ice velocity map of the EAIS using this method, we conduct a series of validation experiments, including comparisons with in-situ measurement, existing historical maps and rock outcrop dataset. Finally, we use the input-output method to estimate mass balance in some regions of EAIS using the generated velocity map.

1. INTRODUCTION

Ice flow velocity on the Antarctic Ice Sheet (AIS) is a significant indicator of its stability and change status under the global climate change conditions (Rignot et al., 2019; The IMBIE Team, 2018). Before 1990s, the ice velocity was mainly measured in the field. Due to the harsh environment in Antarctica, it is difficult to measure the ice velocity, so only in some regions the ice velocity was measured. For example, using modern geodetic observation techniques, Dorrer et al. (1969) measured the ice motions along an east-west and a north-south profile across the Ross Ice Shelf in 1962-1963 and 1965-1966. Manson et al. (2000) used GPS stations in the Lambert - Amery Glacier to obtain ice velocity in 1988-1995. The development of remote sensing technology greatly promotes the study of AIS and achieved the large-scale and high-precision monitoring of ice motion. The InSAR technique make it possible to generate earlier high quality ice flow velocity maps (Jezek, 2002; Rignot et al., 2011a). Most of these maps are produced from SAR images acquired after 1990s due to their availability. However, optical images were acquired since 1960s despite their severe geometric distortions and poor quality. These images were used to generate ice flow velocity maps of the early years using feature tracking techniques from two or more images with a time span from several years to over decade (Chander et al., 2009; Li et al., 2017; Ruffner, 1995; Shen et al., 2018; Wang et al., 2016).

The latest research demonstrates that the East Antarctic Ice Sheet (EAIS) has been in a slightly positive mass balance state (The IMBIE Team, 2018; Rignot et al., 2019), but there exist coastal regions such as Totten Glacier with observed thinning and mass loss accelerating (McMillan et al., 2014; Paolo et al., 2015; Pritchard et al., 2009). Potential drivers of these phenomenon remain less clear (Alley et al., 2005; Shen et al., 2018). Observations from 1992 to 2017 based on comprehensive satellite data show that mass balance of the AIS is estimated to be - 20 ± 15 Gt a^{-1} from Antarctic Peninsula, - 94 ± 27 Gt a^{-1} from West Antarctica, and 5 ± 46 Gt a^{-1} from East Antarctica (The IMBIE Team, 2018). The estimated changes and associated mass balance in East Antarctica are of some degree of uncertainty. Therefore, it is necessary to study this trend in the context of EAIS in a longer period. Three techniques including gravimetry, satellite altimetry and input-output methods can be used to estimate mass balance of AIS (Rignot et al., 2019; The IMBIE Team, 2018). Although three methods differ in their strengths and weaknesses, they lead to similar results when common geographical regions, time intervals, and models of surface mass balance and glacial isostatic adjustment are used (Shepherd et al., 2018). The input-output method is the one that can provide a longest history because of the availability of the long record of optical satellite images.

Since 2012 we have been working on a project that uses ARGON, HEXAGON and Landsat images to produce an East Antarctic velocity map of 1963-1989. Up to this point, we generated a draft velocity map with some regions mapped with multiple periods. However, the map quality and accuracy etc. are being evaluated. We conduct a series of validation experiments to ensure the quality of the ice velocity products. The data we use to perform validation include in-situ measurements, existing historical maps, and rock outcrop dataset. Finally, based on the validated velocity maps, we use the input-output method to estimate mass balance in some regions of EAIS.

* Corresponding author

2. DRAFT ICE VELOCITY MAP OF 1960S TO 1980S

We use historical optical imagery taken before 1990s to extract the ice flow velocity of East Antarctica. ARGON images, HEXAGON images, Landsat images are utilized in this research. Although the image resolution of historical images is relatively low compared with recent satellite images, they provide important information of AIS in earlier years (Kim, 2004; Kim et al., 2001; Li et al., 2017; Wang et al., 2016). HEXAGON images collected by KeyHole-9 (KH-9) were declassified in 2011, with a better ground resolution of ~0.6 m (Fowler, 2013; Gerald, 1997). These images were taken from 1971 to 1986. Multi spectral Scanners (MSS) were carried by Landsat 1-5 since July 1972 and provide images with a ground resolution of 60 m. Thereafter, Thematic Mappers (TM) were equipped on Landsat 4-5 since July 1982 and the resolution of images has been improved to 30 m. A large amount of the images are of poor quality and have not been orthorectified. Based on our previous efforts on improving the quality of these images by denoising, enhancing and ortho-rectifying them (Cheng et al., 2019; Li et al., 2017; Ye et al., 2017), the parallaxes caused by terrain relief are eliminated so that the remain displacements caused by motion of ice can be detected for velocity mapping.

The lack of obvious image features and varying velocities on the surface of EAIS pose challenges for automatic image matching. Initially a set of seed points are selected and matched manually in order to build a triangulated irregular network (TIN), which can serve as the primary control of subsequent feature matching. Within a hierarchical matching strategy at each layer the Shi-Tomasi detector (Shi and Tomasi, 1994) is applied to extract the features and the normalized cross correlation (NCC) technique is used to find corresponding features under the constraint of the TIN model. In the final step, a dense matching is performed to reconstruct the ice velocity field in the form of a grid.

A rigorous procedure is proposed to eliminate the mismatching and evaluate the matching performance by examining velocity magnitudes. By analysing the physical characteristics of topography and glaciers, a set of techniques of detecting the errors in the matched points is carried out, 2 – 3 sigma checking, plane – fitting and error removal, bimodal histogram and others. Furthermore, a median absolute deviation (MAD) filter (Liu et al., 2012) is adopted to eliminate blunders of velocity directions to improve the accuracy.

The produced ice velocity map now covered the entire EAIS except the ring around the south pole and some very small areas without appropriate image coverage. They are ready to be validated for quality control and map compiling.

3. VALIDATION OF THE VELOCITY MAP

3.1 In-situ measurement validation

Due to the harsh climate in Antarctica and the limited ability of field measurements, only a few areas of the ice velocity have been measured by using the field survey methods (theodolites, total stations, GPS). Although the measured data are sparse, they can still provide precious information.

In order to validate our ice velocity generated from historical images, we compare with the field measurements wherever and whenever available and appropriate. For example, we use the field measurement data from Mizuho Plateau (Naruse, 1979), Lambert-Amery Glacier (Allison, 1979; Manson et al., 2000), Zhongshan Station to Dome Argus (Yang et al., 2018) and Scott Coast (Frezzotti et al., 1998). The velocity of the measured points is compared with our velocity within a certain radius which is averaged in a buffer area. In order to ensure the accuracy of the comparison results, the distance between the points to be compared should be short (within a close neighbourhood).

In Mizuho plateau, observations were made by Naruse (1979) in 1969 and 1973-1974. The horizontal vector of ice flow movement at each station can be calculated by the moving distance in two observation periods. The ice velocity extracted from historical images is in good agreement with the ice velocity by the survey of a triangulation network whose sides were by a survey chain. The velocity deviation is within the error range. There is no obvious change detected using these two data sets in Mizuho plateau (72° S).

Allison et al. (1979) made some direct measurements of ice velocity in the Lambert-Amery Glacier from 1960s to 1990s. They are consistent with those from the historical images, with an exception that near a location called “Depot” our velocity differs from the field survey by ~200 m a^{-1}, which appears to be field survey error accumulated along a distance of ~140 km on the ice shelf. Furthermore, Manson et al. (2000) set up GPS stations on the 2500 m contour line of Lambert - Amery Glacier and measured velocity from 1990 to 1995. We compared the ice velocity extracted based on historical images with the results of the repeated GPS measurements; the analysis shows that the ice velocity is relatively consistent.

Yang et al. (2018) used the method of repeated GPS measurements to measure the ice velocity along the route from Zhongshan Station to Dome Argus. The time span is from 2005 to 2016. The ice flow velocity of the two data sets are consistent along the route, with the maximum difference ranging from ~ 4 to ~ 27 m a^{-1} and beyond mapping uncertainty which occurred in the coastal region up to 180 km from Zhongshan Station (GPS velocity higher). Considering the time span, this may indicate that the ice flow velocity in this region increased slightly during this period.

Scott Coast is part of Victoria Land. There are three main glaciers on Scott Coast, namely David Glacier, Reeves Glacier and Priestley Glacier. Frezzotti et al. (1998) made repeated GPS measurements here from 1991 to 1994. The ice velocity obtained from historical images was compared with that from GPS observations. The results show that they are in good agreement, and there is no obvious change in ice velocity during the two observation periods.

In all above analysis if the comparison data have measurements within a period of our historical map time span we require that the velocity differences be within the joint map uncertainty; otherwise both map uncertainty and temporal changes are taken into consideration.

3.2 Existing historical maps validation

Before the 1990s, in addition to the in-situ measurements of ice velocity in some regions of Antarctica, some regions were also measured by using aerial photography and satellite images. We collected ice velocity from Byrd Glacier (Brecher, 1982) and Scott Coast (Frezzotti et al., 1998) based on historical images. In comparison with the existing historical maps, we used ice velocity profiles along main trunks of glaciers.

Brecher (1982) obtained the surface velocity of Byrd Glacier by using two sets of aerial photography from December 1978 to

January 1979. The positions of all measured points on the photographs are determined by a rigorous least-squares adjustment. The linear regression analysis of the ice velocity measured in this study and that measured by Brecher (1982) shows that the results are in good consistency. In addition, we also compared the ice velocity along the centre line of the glacier. The ice velocity measured by Brecher (1982) is faster by up to ~50 m a^{-1} in comparison to our mapping accuracy of ~9 m a^{-1}. Considering the influence of errors of both velocity maps and the map time span difference between 1978-1979 and 1974-1983, the deviation of the ice velocity of Byrd Glacier may be considered tolerable.

Frezzotti et al. (1998) measured ice velocity in David and Drygalski ice tongue regions from 1990 to 1992 based on satellite images. Due to the lack of ground control points, the matching error increases gradually along the Drygalski ice tongue. We obtained two ice velocity maps of 1973-1989 and 1973-1974 at David glacier based on Landsat images. Because the results of ice velocity obtained by feature tracking method based on optical images usually have great uncertainty at the edge of the glacier, we ignore the comparison of ice velocity data at the edge of the glacier. Moreover, we compared the ice velocity of 1973-1988 with that extracted by Frezzotti et al. (1998) at the centre line of David glacier. The results show that the David Glacier is basically stable during this period. Moreover, Frezzotti et al. (1998) obtained the ice velocity of Reeves Glacier using SPOT image in December 1988 and Landsat image in January 1992. In the Reeves Glacier, we extracted the ice velocity of 1972-1989 and 1988-1989. In Priestley Glacier, we and Frezzotti et al. (1998) extracted the ice velocity from 1972-1989 and 1990-1992 using Landsat images, respectively. The results show that the ice velocity on Reeves Glacier and Priestley Glacier is in good agreement with that extracted by Frezzotti et al. (1998).

3.3 Rock outcrop validation

The rock outcrop validation is one of the important validations of ice velocity extracted from historical images. We validated the velocity of rock outcrop distribution regions by using rock outcrop dataset (Burton-Johnson et al., 2016), which is available from the SCAR Antarctic Digital Database (http://www.add.scar.org). The rock outcrop dataset is obtained by using a method of automatically distinguishing snow and rocks from Landsat 8 images. For most areas south of 82°40′S that are not covered by Landsat 8 imagery, the previous version of the rock outcrop dataset (Thomson and Cooper, 1993) is used. The exposed rock covers an area of about 21745 km^2, accounting for 0.18% of the total area of Antarctica.

Considering the quality of historical image and other factors, we mainly verify whether the velocity of matched points in outcrop area is less than 10 m a^{-1} (within our mapping capability). In some cases where only a small number of ice velocity matched points are available, the interpolation may produce slightly higher velocity (more than 10 m a^{-1}). Then the areas may be revised by measuring additional velocity points.

Zwally et al. (2012) divided the AIS into 27 basins, including basins 2 to 17 of the East Antarctica, basin 1 and basin 18 to 23 of the West Antarctica, and basin 24 - 27 of the Antarctic Peninsula. In this paper, we take basin 3 (Figure 1) as an example to verify and analyse the rock outcrop region. There are 513 matched points in the rock outcrop region of basin 3. The mean value of these matched points is 5.6 m a^{-1}, the maximum velocity is 9.8 m a^{-1}, and the minimum velocity is 0. It shows that the velocity differences with the outcrop database are within the mapping uncertainty, 99 % less than 10 m a^{-1} and 1 % greater than10 m a^{-1}, but within mapping uncertainty.

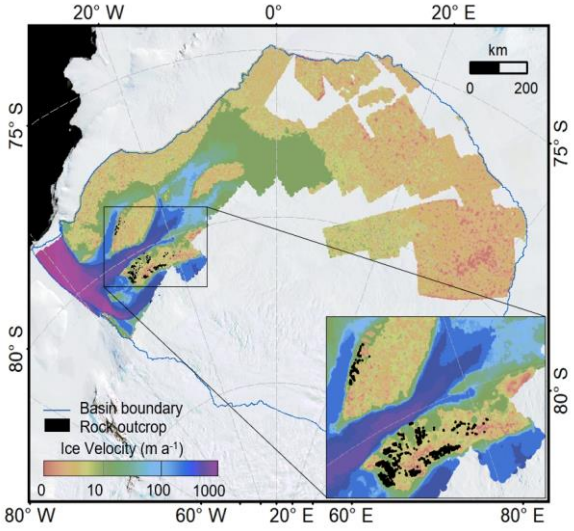

Figure 1. Rock outcrop distribution and ice velocity of basin 3, overlaid on the The Landsat image mosaic of Antarctica (Bindschadler et al., 2008)

Up to this point, the rock outcrop verification has been completed in most regions of the EAIS.

4. CALCULATION OF MASS BALANCE

4.1 Ice discharge

Ice discharge refers to the ice mass or volume per unit time flowing across the grounding line (GL) of the ice sheet. The location of grounding is vital because it determines the position of the flux gates. In consideration of the distribution of ice thickness data (Fretwell et al., 2013) and the uncertainty of the ice velocity map, we modify the gate locations from the grounding line (Rignot et al., 2011b) to new flux gates supported by high quality ice thickness data (Gardner et al., 2018).

We sample along the flux gates (the spacing between the sampling points is ~ 280 meters), in order to obtain sufficient ice thickness and velocity data. Assuming that the ice velocity does not change in the vertical gradient, we calculate ice flux (F) cross the flux gates. Thereafter, a correction ($Corr_{GL\text{-}Gate}$) has been applied to compute ice discharge from ice flux, which is the surface mass balance between the flux gates and the grounding line. The $Corr_{GL\text{-}Gate}$ is calculated using the RACMO2.3 p2 regional climate model (van Wessem et al., 2018) at 27 km resolution and averaged over the 1979-1989 period. According to the principle of conservation of mass (Morlighem et al., 2011), ice discharge (D) is equal to the sum of F and $Corr_{GL\text{-}Gate}$.

4.2 Mass balance

Furthermore, SMB from RACMO 2.3 p2 (1979-1989) is used as the input component. Due to the time range of the regional climate model (van Wessem et al., 2018), we use the basin-wide average SMB from 1979 to 1989 to represent the longer-term surface mass balance. Based on the mentioned input and output components, we are now able to obtain the mass balance of the EAIS.

The mass balance of basin 3, basin 4, basin 5, basin 6, Totten Glacier, Fimbul region and Byrd Glacier, were calculated by

using the input-output method according to the ice velocity map generated in this study. We compared the results of mass balance based on the velocity map obtained in this study with those based on other velocity products and other related results, and then analysed reasons for the change of mass balance in combination with ice shelf front, climate model and other factors.

The mass balance of basin 3, basin 4, basin 5 and basin 6 are all positive, indicating that these basins were in the state of accumulation in the 1960s-1980s.Totten Glacier is one of the most active regions in East Antarctica. In this study, we used ARGON images and Landsat images to obtain velocity maps of the Totton Glacier from 1963 to 1973, 1973 to 1989, and from March to November 1989. The velocity of the ice shelf section fluctuated from 1963 to 1989, but velocity of the grounded ice was still in a relatively stable state, thus the ice flux of Totten Glacier did not change significantly. Meanwhile, we estimated the ice velocity in three periods of 1963-1975, 1973-1987 and 1985-1987 on the Fimbul region, and then the velocity maps were compared with the published velocity products from 2007 to 2008 (Mouginot et al., 2017). The results show that there was no significant change in the ice velocity from 1963 to 2008. The result suggests a slightly positive mass balance trend. We also estimated the ice velocity and mass balance of Byrd Glacier from 1963 to 2020. The result shows that although the velocity of Byrd Glacier fluctuated in the past 60 years, the fluctuation range was small. The variation of velocity may be affected by the activities of the subglacial drainage system and the dynamics of the Ross Ice Shelf. In addition, the Byrd Glacier was in a positive mass balance state from 1963 to 2020.

5. CONCLUSIONS

In this research, we validate the draft ice velocity map based on the historical images from 1960s to 1980s, and use the input-output method to estimate the mass balance of some regions in EAIS based on the generated ice velocity map.

The results of the validation using three types of validation data sets indicate that the ice velocity obtained in this study is in good agreement with the velocity of the compared data in EAIS from 1960s to 1980s. We have then calculated the mass balance of some regions in EAIS based on the generated velocity map by using the input-output method. The results of mass balance from basin 3 to basin 6 show that these regions are in the state of accumulation during the period of 1960s-1980s, which is consistent with the positive mass balance in the EAIS. Moreover, the velocity of several typical regions including Totten Glacier, Fimbul region and Byrd Glacier in different time periods before 1990s were estimated. Long-term characteristics of ice velocity in these regions were analysed.

In the future work, we will analyse the dynamic characteristics of the main glaciers in combination with the published velocity products, and we will use the input-output method to estimate the mass balance of EAIS from 1960s to 1980s based on generated velocity map, which makes it possible to analyse the ice velocity and mass balance change since 1960s and to understand the early changes of EAIS.

ACKNOWLEDGEMENTS

This work has been supported by the National Key Research & Development Program of China (No. 2017YFA0603102) and the National Science Foundation of China (41730102).

REFERENCES

Alley, R.B., Clark, P.U., Huybrechts, P., Joughin, I., 2005. Ice-sheet and sea-level changes. Science 310, 456–460. https://doi.org/10.1126/science.1114613

Allison, I., 1979. The mass budget of the Lambert Glacier drainage basin, Antarctica. Journal of Glaciology 22, 223–235.

Bindschadler, R., Vornberger, P., Fleming, A., Fox, A., Mullins, J., Binnie, D., Paulsen, S., Granneman, B., Gorodetzky, D., 2008. The Landsat Image Mosaic of Antarctica. Remote Sensing of Environment 112, 4214–4226. https://doi.org/10.1016/j.rse.2008.07.006

Brecher, H., 1982. Photographic determination of surface velocities and elevations on Byrd Glacier. Antarct. J. US 17, 79–81.

Burton-Johnson, A., Black, M., Fretwell, P.T., Kaluza-Gilbert, J., 2016. An automated methodology for differentiating rock from snow, clouds and seain Antarctica from Landsat 8 imagery: a new rock outcrop map and areaestimation for the entire Antarctic continent. The Cryosphere 10, 1665–1677. https://doi.org/10.5194/tc-10-1665-2016

Chander, G., Markham, B.L., Helder, D.L., 2009. Summary of current radiometric calibration coefficients for Landsat MSS, TM, ETM+, and EO-1 ALI sensors. Remote Sensing of Environment 113, 893–903. https://doi.org/10.1016/j.rse.2009.01.007

Cheng, Y., Li, X., Qiao, G., Ye, W., Huang, Y., Li, Y., Wang, K., Tian, Y., Tong, X., Li, R., 2019. ICE FLOW VELOCITY MAPPING OF EAST ANTARCTICA FROM 1963 TO 1989. Int. Arch. Photogramm. Remote Sens. Spatial Inf. Sci. XLII-2/W13, 1735–1739. https://doi.org/10.5194/isprs-archives-XLII-2-W13-1735-2019

Dorrer, E., Hofmann, W., Seufert, W., 1969. Geodetic Results of the Ross Ice Shelf Survey Expeditions, 1962–63 and 1965–66. Journal of Glaciology 8, 67–90. https://doi.org/10.3189/S0022143000020773

Fowler, M.J.F., 2013. Declassified Intelligence Satellite Photographs, in: Hanson, W.S., Oltean, I.A. (Eds.), Archaeology from Historical Aerial and Satellite Archives. Springer, New York, NY, pp. 47–66. https://doi.org/10.1007/978-1-4614-4505-0_4

Fretwell, P., Pritchard, H.D., Vaughan, D.G., Bamber, J.L., Barrand, N.E., Bell, R., Bianchi, C., Bingham, R.G., Blankenship, D.D., Casassa, G., Catania, G., Callens, D., Conway, H., Cook, A.J., Corr, H.F.J., Damaske, D., Damm, V., Ferraccioli, F., Forsberg, R., Fujita, S., Gim, Y., Gogineni, P., Griggs, J.A., Hindmarsh, R.C.A., Holmlund, P., Holt, J.W., Jacobel, R.W., Jenkins, A., Jokat, W., Jordan, T., King, E.C., Kohler, J., Krabill, W., Riger-Kusk, M., Langley, K.A., Leitchenkov, G., Leuschen, C., Luyendyk, B.P., Matsuoka, K., Mouginot, J., Nitsche, F.O., Nogi, Y., Nost, O.A., Popov, S.V., Rignot, E., Rippin, D.M., Rivera, A., Roberts, J., Ross, N., Siegert, M.J., Smith, A.M., Steinhage, D., Studinger, M., Sun, B., Tinto, B.K., Welch, B.C., Wilson, D., Young, D.A., Xiangbin, C., Zirizzotti, A., 2013. Bedmap2: improved ice bed, surface and thickness datasets for Antarctica. The Cryosphere 7, 375–393. https://doi.org/10.5194/tc-7-375-2013

Frezzotti, Ma., Capra, A., Vittuari, L., 1998. Comparison between glacier ice velocities inferred from GPS and sequential satellite images. Annals of Glaciology 27, 54–60. https://doi.org/10.3189/1998AoG27-1-54-60

Gardner, A.S., Moholdt, G., Scambos, T., Fahnstock, M., Ligtenberg, S., Van Den Broeke, M., Nilsson, J., 2018. Increased West Antarctic and unchanged East Antarctic ice discharge over the last 7 years. The Cryosphere 12, 521–547.

Gerald, K., 1997. Haines. Critical to US Security: the development of the GAMBIT and HEXAGON satellite reconnaissance system. National Reconnaissance Office.

Jezek, K.C., 2002. RADARSAT-1 Antarctic Mapping Project: change-detection and surface velocity campaign. Annals of Glaciology 34, 263–268.

Kim, K.-T., 2004. Satellite mapping and automated feature extraction: Geographic information system-based change detection of the Antarctic Coast (PhD Thesis). The Ohio State University.

Kim, K.T., Jezek, K.C., Sohn, H.G., 2001. Ice shelf advance and retreat rates along the coast of Queen Maud Land, Antarctica. Journal of Geophysical Research: Oceans 106, 7097–7106.

Li, R., Ye, W., Qiao, G., Tong, X., Liu, S., Kong, F., Ma, X., 2017. A New Analytical Method for Estimating Antarctic Ice Flow in the 1960s From Historical Optical Satellite Imagery. IEEE Transactions on Geoscience and Remote Sensing 55, 2771–2785. https://doi.org/10.1109/TGRS.2017.2654484

Liu, H., Wang, L., Tang, S.-J., Jezek, K.C., 2012. Robust multi-scale image matching for deriving ice surface velocity field from sequential satellite images. International journal of remote sensing 33, 1799–1822.

Manson, R., Coleman, R., Morgan, P., King, M., 2000. Ice velocities of the Lambert Glacier from static GPS observations. Earth, planets and space 52, 1031–1036.

McMillan, M., Shepherd, A., Sundal, A., Briggs, K., Muir, A., Ridout, A., Hogg, A., Wingham, D., 2014. Increased ice losses from Antarctica detected by CryoSat-2. Geophysical Research Letters 41, 3899–3905.

Morlighem, M., Rignot, E., Seroussi, H., Larour, E., Dhia, H.B., Aubry, D., 2011. A mass conservation approach for mapping glacier ice thickness. Geophysical Research Letters 38. https://doi.org/10.1029/2011GL048659

Mouginot, J., Rignot, E., Scheuchl, B., Millan, R., 2017. Comprehensive Annual Ice Sheet Velocity Mapping Using Landsat-8, Sentinel-1, and RADARSAT-2 Data. Remote Sensing 9, 364. https://doi.org/10.3390/rs9040364

Naruse, R., 1979. Studies on the Ice Sheet Flow and Local Mass Budget in Mizuho Plateau, Antarctica. Contributions from the Institute of Low Temperature Science 28, 1–54.

Paolo, F.S., Fricker, H.A., Padman, L., 2015. Volume loss from Antarctic ice shelves is accelerating. Science 348, 327–331. https://doi.org/10.1126/science.aaa0940

Pritchard, H.D., Arthern, R.J., Vaughan, D.G., Edwards, L.A., 2009. Extensive dynamic thinning on the margins of the Greenland and Antarctic ice sheets. Nature 461, 971–975. https://doi.org/10.1038/nature08471

Rignot, E., Mouginot, J., Scheuchl, B., 2011a. Ice Flow of the Antarctic Ice Sheet. Science 333, 1427–1430. https://doi.org/10.1126/science.1208336

Rignot, E., Mouginot, J., Scheuchl, B., 2011b. Antarctic grounding line mapping from differential satellite radar interferometry. Geophysical Research Letters 38. https://doi.org/10.1029/2011GL047109

Rignot, E., Mouginot, J., Scheuchl, B., van den Broeke, M., van Wessem, M.J., Morlighem, M., 2019. Four decades of Antarctic Ice Sheet mass balance from 1979–2017. Proc Natl Acad Sci USA 116, 1095–1103. https://doi.org/10.1073/pnas.1812883116

Ruffner, K.C., 1995. Corona: America's first satellite program. History Staff, Center for the Study of Intelligence, Central Intelligence Agency.

Shen, Q., Wang, H., Shum, C.K., Jiang, L., Hsu, H., Dong, J., 2018. Recent high-resolution Antarctic ice velocity maps reveal increased mass loss in Wilkes Land, East Antarctica. Scientific Reports 8. https://doi.org/10.1038/s41598-018-22765-0

Shepherd, A., Fricker, H.A., Farrell, S.L., 2018. Trends and connections across the Antarctic cryosphere. Nature 558, 223–232. https://doi.org/10.1038/s41586-018-0171-6

Shi, J., Tomasi, 1994. Good features to track, in: 1994 Proceedings of IEEE Conference on Computer Vision and Pattern Recognition. Presented at the 1994 Proceedings of IEEE Conference on Computer Vision and Pattern Recognition, pp. 593–600. https://doi.org/10.1109/CVPR.1994.323794

The IMBIE Team, 2018. Mass balance of the Antarctic Ice Sheet from 1992 to 2017. Nature 558, 219–222. https://doi.org/10.1038/s41586-018-0179-y

Thomson, J.W., Cooper, A.P.R., 1993. The SCAR Antarctic digital topographic database. Antarctic Science 5, 239–244. https://doi.org/10.1017/S095410209300032X

van Wessem, J.M., van de Berg, W.J., Noël, B.P.Y., van Meijgaard, E., Amory, C., Birnbaum, G., Jakobs, C.L., Krüger, K., Lenaerts, J.T.M., Lhermitte, S., Ligtenberg, S.R.M., Medley, B., Reijmer, C.H., van Tricht, K., Trusel, L.D., van Ulft, L.H., Wouters, B., Wuite, J., van den Broeke, M.R., 2018. Modelling the climate and surface mass balance of polar ice sheets using RACMO2 – Part 2: Antarctica (1979–2016). The Cryosphere 12, 1479–1498. https://doi.org/10.5194/tc-12-1479-2018

Wang, S., Liu, H., Yu, B., Zhou, G., Cheng, X., 2016. Revealing the early ice flow patterns with historical Declassified Intelligence Satellite Photographs back to 1960s. Geophysical Research Letters 43, 5758–5767. https://doi.org/10.1002/2016GL068990

Yang, Y., Ke, H., Wang, Z., Li, F., Ding, M., Sun, B., Jin, B., Wang, L., Ai, S., 2018. Decadal GPS-derived ice surface velocity along the transect from Zhongshan Station to and around Dome Argus, East Antarctica, 2005–16. Annals of Glaciology 59, 1–9. https://doi.org/10.1017/aog.2018.3

Ye, W., Qiao, G., Kong, F., Ma, X., Tong, X., Li, R., 2017. Improved Geometric Modeling of 1960s KH-5 ARGON Satellite

Images for Regional Antarctica Applications. Photogrammetric Engineering and Remote Sensing 83, 477–491.

Zwally, H.J., Giovinetto, M.B., Beckley, M.A., Saba, J.L., 2012. Antarctic and Greenland drainage systems, GSFC cryospheric sciences laboratory.